Nordesferriferrithiocin. Comparative Coordination Chemistry of a Prospective Therapeutic Iron Chelating Agent[1]

Klaus Langemann, Daniel Heineke, Stefan Rupprecht, and Kenneth N. Raymond*

Department of Chemistry, University of California at Berkeley Berkeley, California 94720

Received February 22, 1996[⊗]

Nordesferriferrithiocin, $NDFFTH_2$, is a derivative of the siderophore desferriferrithiocin, $DFFTH_2$, in which the methyl group is substituted by a hydrogen atom. Both compounds show high oral activity as possible drugs for the treatment of iron overload. While $DFFTH_2$ is significantly toxic, $NDFFTH_2$ exhibits a lower toxicity and offers a much better therapeutic window than other orally active iron chelators. In this study, complexes of $DFFTH_2$ and $NDFFTH_2$ with various trivalent metals have been synthesized and characterized. Five isomers (the maximum possible) have been observed in the case of $[Co(DFFT)_2]^-$ in solution, as proved by ^{1}H-NMR measurements. Although normally labile, complexes of Al^{3+} ($[Al(DFFT)_2]^-$) have been separated by HPLC. In general, $DFFTH_2$ forms kinetically inert complexes whereas complexes of $NDFFTH_2$ tend to isomerize quickly in solution, as indicated by CD spectroscopy of separated HPLC fractions of $[Cr(NDFFT)_2]^-$. The most stable isomers of the aluminum complexes of both ligands have been characterized by X-ray crystallography; K[Al-(DFFT)$_2$] crystallizes from methanol/diethyl ether in the orthorhombic space group $P2_12_12$ with $a = 11.238(3)$ Å, $b = 31.719(11)$ Å, $c = 7.684(2)$ Å, $V = 2739.2(24)$ Å^3, and $Z = 4$. This isomer has the mer-(N,O-Λ)(*S*,*S*) configuration, while K[Al(NDFFT)$_2$] crystallizes from methanol/diethyl ether in the space group $P6_1$ ($a = 21.269(8)$ Å, $c = 9.643(3)$ Å, $V = 3777.8(42)$ Å^3, $Z = 6$) and has the same coordination geometry. The solution thermodynamics of the Al^{3+}, Ga^{3+}, and Fe^{3+} complexes have been studied by spectrophotometric titration. The stability constants (log *K*) are 23.6(1), 29.2(3), and 31.04(3), respectively, for the $DFFTH_2$ complexes and 22.0-(1), 27.8(2), and 29.09(3), respectively, for the $NDFFTH_2$ complexes. Cyclic voltammograms of both iron complexes have been recorded in water at a carbon disk working electrode and in DMF at a graphite working electrode. The reduction waves measured in DMF indicate no reversibility whereas in water a quasi-reversible reduction is observed. The reduction potentials ($E_{1/2}$'s) in water are −166 mV for $[Fe(DFFT)_2]^-$ and −97 mV for $[Fe(NDFFT)_2]^-$ versus NHE. These potentials are well in the range for biological reductants, which makes possible an *in vivo* reduction mechanism for the iron removal from the siderophore.

Introduction

The essential role of iron in the chemistry of life and that element's unavailability, even though widely abundant, is well-known.[2−6] To solubilize and transport iron, microorganisms excrete siderophores.[5−8] In numerous studies it has been shown that microbial receptors show remarkable selectivity for geometry and chirality at the metal center;[9] hence the identification and characterization of the different isomers of the metal complex siderophores are significant. Another significant issue is the mechanism of iron removal from the siderophore, to make iron available to the cell. Since the stability constants of the ferric complexes are as much as 10^{30}−10^{49}, microorganisms must have powerful tools for iron removal. Several mechanisms have been found or proposed. The simplest is the reduction of Fe(III) to Fe(II) (which results in dissociation of the complex). Hence the redox potentials of various siderophores have been studied. The electrochemistry is also of significance for free radical tissue damage caused by iron. Free Fe^{2+} is hazardous: the catalytic activity of iron in one-electron redox reactions can generate harmful oxygen radicals.[4,9]

Siderophores are either prototypes for, or actually used as, chelating agents for therapeutic iron chelators in clinical use. Desferrioxamine (DFO) (Desferal, the methanesulfonate derivative of DFO) is employed clinically as an effective drug for the treatment of diseases such as hemosiderosis and β-thalassemia, or accidental iron poisoning.[10] It has also been studied in several other possible medical applications. However its role has remained primarily as an iron chelator, where Desferal still has some serious limitations. It is kinetically slow to remove iron from the body, and the oral effectiveness is so low[11] that the drug has to be administered by injection. Significant neurotoxicity has been observed in patients receiving continuous intravenous infusions of Desferal.[10] Thus, there has remained

* To whom correspondence should be addressed.

⊗ Abstract published in *Advance ACS Abstracts,* August 15, 1996.

(1) Coordination Chemistry of Microbial Iron Transport. 59. For part 58, see ref 8.
(2) Theil, E. C.; Raymond, K. N. In *Bioinorganic Chemistry*; University Science Books: Mill Valley, CA, 1994; pp 1−37.
(3) Wrigglesworth, J. M.; Baum, J. *The Biochemical Function of Iron in Biochemistry and Medicine*; Academic Press: London, 1980, Vol. II.
(4) Telford, J. R.; Raymond, K. N. In *Comprehensive Supramolecular Chemistry*; Lehn, J. M., Ed.; Pergamon Press: New York, 1995; Vol. 1.
(5) Raymond, K. N.; Telford, J. R. In *Bioinorganic Chemistry: An Inorganic Perspective of Life*; NATO ASI Series 459; Kluwer Academic Publishers: Dordrecht, The Netherlands, 1995; pp 25−37.
(6) *CRC Handbook of Microbial Iron Chelates*; Winkelmann, G., Ed.; CRC Press: Boca Raton, FL, 1991.
(7) Matzanke, B. F.; Müller-Matzanke, G.; Raymond, K. N. In *Iron Carriers and Iron Proteins*; VCH Publishers: New York, 1989; pp 1−121.
(8) Telford, J. R.; Leary, J. A.; Tunstad, L. M. G.; Byers, B. R.; Raymond, K. N. *J. Am. Chem. Soc.* **1994**, *116*, 4499.
(9) Aisen, P. In *Iron Metabolism*; Elsevier: Amsterdam, 1977; Vol. 51 (New Series), p 1.
(10) Pippard, M. J. *The Development of Iron Chelators for Clinical Use*; CRC Press Inc.: Boca Raton, FL, 1994.
(11) Schnebli, H. P.; Hassan, I.; Hamilton, K. O.; Lynch, S.; Jin, Y.; Nick, H. P.; Peter, H. H.; Junker Walter, U.; Ziel, R.; Khanna, S. C.; Dean, R.; Bergeron, R. J. *The Development of Iron Chelators for Clinical Use*; CRC Press Inc.: Boca Raton, FL, 1994.

S0020-1669(96)00185-1 CCC: $12.00

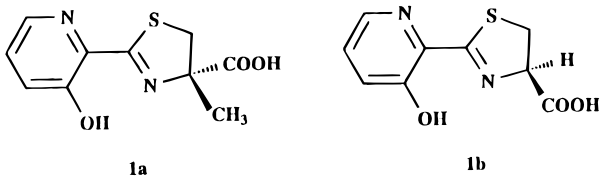

Figure 1. Structures of the naturally-occurring siderophore desferriferrithiocin, **1a** ($DFFTH_2$), and the synthetic siderophore nordesferriferrithiocin, **1b** ($NDFFTH_2$).

a demand for highly efficient orally active iron chelators which are suitable for clinical administration. Unfortunately, while most orally active iron chelators are bi- or tridentate,[11] the bidentate siderophores in general are too weak as sequestering agents for Fe(III) at physiological pH.[12] One recent new prospect has been the siderophore desferriferrithiocin (**1a**) (Figure 1), first isolated from *Streptomyces antibioticus*.[13]

Desferriferrithiocin (($DFFTH_2$) is a tridentate ligand, coordinating via the phenolate oxygen atom, the nitrogen atom in the thiazoline ring, and the carboxylate oxygen atom. Like two other recently identified siderophores, anguibactin[14] and pyochelin,[15,16] $DFFTH_2$ contains a thiazoline ring. The siderophore is chiral with an *S* absolute configuration at the quaternary carbon atom; in theory it can form five different octahedral metal bis complex isomers that are not eliminated by the steric constraints of the ligand. They all have C_2 symmetry; three isomers are facial and two are meridional. Since the ligand is chiral, each of the complexes is chiral; the two meridional isomers are diastereomers. An IUPAC[17] nomenclature for these two isomers (A, anti clockwise; C, clockwise) has been introduced. A less formal but descriptive nomenclature for all of the isomers is presented in Figure 2.[18,19]

The formation constants of the 1:1 and 2:1 complexes of $DFFTH_2$ with several metal ions have been reported,[20] and the characterization of a 1:1 copper complex has been described.[21] We have earlier reported characterization of the 2:1 complexes of $DFFTH_2$ with Cr^{3+} and Co^{3+}.[22] While $DFFTH_2$ was found to be highly orally active, as a possible drug for iron decorporation it proved to be unacceptably toxic. However relatively small modifications of $DFFTH_2$ profoundly altered the toxicity profile.[11] Replacement of the methyl group at the chiral carbon atom with a hydrogen atom yielded a less lipophilic, low-toxicity ligand: nordesferriferrithiocin ($NDFFTH_2$, **1b**, Figure 1). Here the chiral carbon atom in the thiazoline ring has an *R* absolute configuration. The same constraints and nomenclature for the five possible isomers of $DFFTH_2$ apply to $NDFFTH_2$, but one has to account for the different configuration of the ligands (replace *SS* with *RR*). It has been found that $NDFFTH_2$ is more effective in iron removal from monkeys than Desferal and offers a better therapeutic window than any other orally active iron chelator.[23]

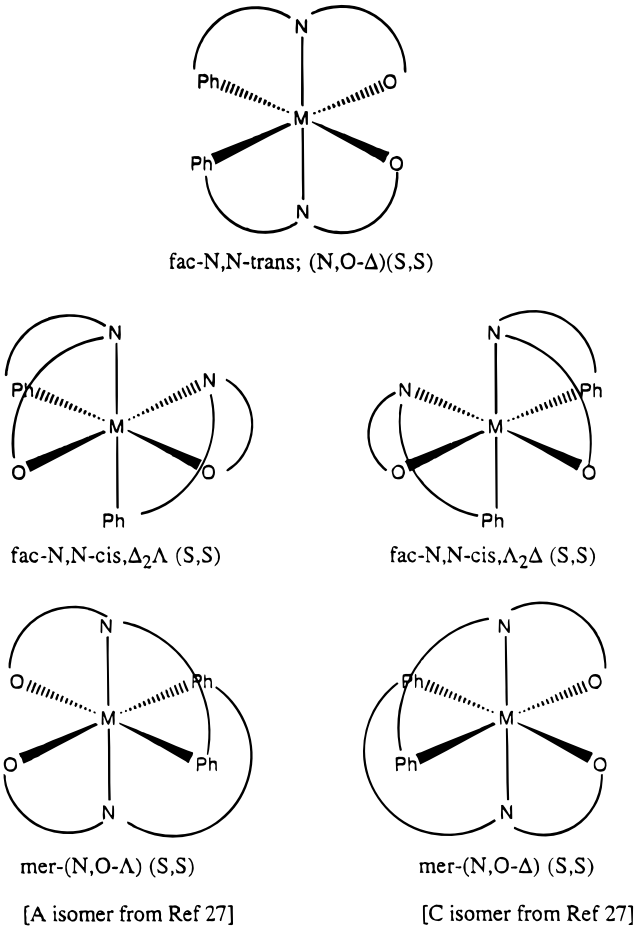

Figure 2. The five possible isomers of $[M(DFFT)_2]^-$ and their nomenclature (O refers to the carboxylic oxygen atom; Ph refers to the phenolate oxygen atom). See ref 22 for a discussion of the isomer nomenclature.

This work describes the preparation and characterization of complexes of both the siderophore and its derivative, $DFFTH_2$ and $NDFFTH_2$, with several trivalent metal ion analogs of Fe(III). The assignment of the different isomers of the complexes has been achieved with several spectroscopic techniques. A detailed description of the thermodynamic behavior of the labile complexes of Al^{3+}, Ga^{3+}, and Fe^{3+} in solution and a structural characterization in the solid state of both aluminum complexes are also presented. The iron complexes have been studied by cyclic voltammetry. In all these studies, the primary goal is to compare the properties of these closely related ligands, $DFFTH_2$ and $NDFFTH_2$.

Experimental Section

General Procedures. Desferriferrithiocin and nordesferriferrithiocin (both as the monohydrates) were a generous gift from Ciba Geigy. Acetone was allowed to stand overnight over P_2O_5 and distilled. It was later dried over 3 Å molecular sieves and distilled prior to use. Reactive starting materials $Na_3[Co(CO_3)_3]\cdot 3H_2O$ and $CrCl_3\cdot 3THF$ were prepared according to common literature procedures.[24,25] Triethylamine was distilled from CaH_2 prior to use. All other starting materials were, unless otherwise specified, commercially available reagents and were used as received. ^{1}H-NMR spectra were recorded on a 300 MHz FT Bruker instrument. Mass spectra were recorded by the UCB Mass Spectrometer Facility. Elemental analyses were performed by the UCB

(12) Raymond, K. N.; Xu, J. In *The Development of Iron Chelators for Clinical Use*; CRC Press, Inc.: Boca Raton, FL, 1994; pp 307−327.
(13) Naegeli, H. U.; Zähner, H. *Helv. Chim. Acta* **1980**, *63*, 1400.
(14) Jalal, M. A. F.; Hossain, M. V.; van der Helm, P.; Sanders-Loehr, J.; Actis, L. A.; Crosa, J. H. *J. Am. Chem. Soc.* **1989**, *111*, 292−296.
(15) Cox, D. D.; Rinehart, K. L.; Moore, M. L.; Cook, J. C. *Proc. Natl. Acad. Sci. U.S.A.* **1981**, *78*, 4256.
(16) Ankenbauer, R. G.; Toyokani, T.; Staley, A.; Rinehart, K. L., Jr.; Cox, C. *J. Bacteriol.* **1988**, *170*, 5344−5351.
(17) *Inorg. Chem.* **1970**, *9*, 1.
(18) Brorson, M.; Damhus, T.; Schäffer, C. E. *Inorg. Chem.* **1983**, *22*, 1569−1573.
(19) von Zelewsky, A. Personal communication.
(20) Anderegg, G.; Räber, M. *J. Chem. Soc., Chem. Commun.* **1990**.
(21) Schechinger, T.; Hiller, W.; Mauble, C.; Straehle, J.; Weser, U. *Biol. Met.* **1988**, *1*, 112−116.
(22) Hahn, F. E.; McMurry, T. J.; Hugi, A.; Raymond, K. N. *J. Am. Chem. Soc.* **1990**, *112*, 1854−1860.
(23) Bergeron, R. J.; Liu, C. Z.; McManis, J. S.; Xia, M. X. B.; Algee, S. E.; Wiegand, J. *J. Med. Chem.* **1994**, *37*, 1411−1417.
(24) Bauer, H. F.; Drinkard, W. C. *J. Am. Chem. Soc.* **1960**, *82*, 5031−5032.
(25) Angelici, R. J. *Synthesis and Techniques in Inorganic Chemistry*; W. B. Saunders Co.: Philadelphia, PA, 1969.

Microanalysis Facility. Vis/UV spectra were recorded on a Hewlett-Packard HP8450A instrument using 1 cm path length quartz cells; CD spectra were obtained using a Jasco J500-C spectrometer and 1 cm quartz cuvettes. Isomer separation was achieved by high-performance liquid chromatography (HPLC) using a Hamilton PRP-1 semipreparative column (25 × 1 cm). All pH measurements were performed using a Fisher Accumet pH meter (Model 825MP) and a glass electrode which was calibrated with commercially available buffer solutions for hydrogen ion concentration, not activity. Melting points were determined with a Mel-Temp laboratory device and are uncorrected. Solutions were aqueous unless otherwise indicated.

Syntheses. Preparation of K[Al(DFFT)$_2$]·H$_2$O (2a). $AlCl_3$ (anhydrous, 0.16 g, 1.2 mmol) was dissolved in water, and the pH was adjusted to 5.5 with 0.5 M KOH. The white precipitate was centrifuged and washed several times with water until the supernatant gave no further reaction with $AgNO_3$ solution. A slurry of the purified $Al(OH)_3$ in 5 mL of water was added to a solution of 0.381 g (1.6 mmol) of desferriferrithiocin ($DFFTH_2$, **1a**) and 8 mL of a 0.1 M KOH solution (0.8 mmol) in 10 mL of water. The reaction mixture was stirred at room temperature for 48 h in the dark. After filtration from the excess $Al(OH)_3$, the solvent was removed in vacuo to give 290 mg (34%) of the raw product as a yellow powder. The residue was dissolved in methanol, applied to a Sephadex LH-20 column (25 × 2 cm), and eluted with methanol. A yellow band was collected. The solvent was removed in vacuo. The sample was characterized by ^{1}H-NMR, its FAB mass spectrum, and microanalysis. Anal. Calcd (found) for $KAlC_{20}H_{18}N_4O_7S_2$: C, 43.16 (43.66); H, 3.23 (3.22); N, 10.06 (10.05); Al, 4.8 (5.1). The ^{1}H-NMR spectrum indicated that there are three isomers in solution in the ratio of 1:0.23:0.19. Negative ion FABMS: *m*/*e* (relative abundance) 499 (100%), 538 (60%). The complex decomposes between 321 and 324 °C. These isomers exchange slowly enough that separation was achieved by HPLC; 20 mg of the mixture of Al(III) complexes dissolved in 0.2 mL of water was injected into the column. An ion-free solvent system (solvent A, water; solvent B, methanol) was used with the following gradient: 10−55% B (1%/min). The flow rate was 5 mL/min. The peak eluting at 10.3 min was identified as an oxidation product of the ligand and was discarded. The two peaks eluting at 34.0 and 38.0 min were collected, lyophilized, and characterized by ^{1}H-NMR. The first fraction showed a set of signals of isomer A and trace amounts of another isomer. The second fraction contained a mixture of all three isomers observed in the crude product. The pure isomer A was also characterized by X-ray diffraction and vis/UV measurements.

Preparation of K[Al(NDFFT)$_2$]·3H$_2$O (2b). Pure $Al(OH)_3$ was prepared as described above using 32 mg (0.24 mmol) of $AlCl_3$ (anhydrous). A slurry of $Al(OH)_3$ in 10 mL of water was added to a solution of 105 mg (0.43 mmol) of nordesferriferrithiocin ($NDFFTH_2$, **1b**) and 0.215 mmol of KOH in 15 mL of water. The mixture was stirred for 40 h at room temperature. The solvent was removed in vacuo, the residue was dissolved in methanol, and the solution was applied to a Sephadex LH-20 column (20 × 1 cm) and eluted with methanol. Removal of the solvent followed by lyophilization gave 105 mg (48%) of a yellowish solid, which was characterized by ^{1}H-NMR, FABMS, and elemental analysis. Anal. Calcd (found) for $KAlC_{18}H_{18}N_4O_9S_2$: C, 38.30 (38.02); H, 3.19 (3.21); N, 9.92 (9.59); Al, 4.9 (5.3). The recorded ^{1}H-NMR spectrum indicated that there were at least two different species in solution. Negative ion FABMS: *m*/*e* (relative abundance) 471 (92%), 510 (10%). Decomposition of the complex occurs between 310 and 320 °C.

Isomer separation was attempted by HPLC with various solvent gradients at a flow rate of 5 mL/min. The peak eluting between 38 and 40 min was collected. The ^{1}H-NMR spectrum showed two sets of signals of two isomers in a ratio of 1:0.44. However, it was impossible to separate the isomers, presumably due to faster interconversion. Single crystals were grown from the solution containing the mixture of the two isomers; X-ray diffraction indicated that the A isomer is the sole product.

Preparation of K[Ga(DFFT)$_2$]·4H$_2$O (3a). Gallium (83.6 mg, 1.2 mmol) was dissolved in concentrated hydrochloric acid. The pH was adjusted to 6.5 with 0.5 M KOH, and the white precipitate was removed by centrifugation and washed repeatedly with water until free of chloride. A slurry of the purified $Ga(OH)_3$ in 10 mL of water was added in portions to a solution of 410.0 mg (1.6 mmol), $DFFTH_2$, **1a**, in 15 mL of water and 8.0 mL of a 0.1 M KOH solution (0.8 mmol). The reaction mixture was stirred for 36 h at room temperature. The solvent was removed in vacuo, and the residue applied to a Sephadex LH-20 column (25 × 2 cm) and eluted with methanol. The solvent was removed, giving 320 mg of a brown-yellow solid. To separate the ligand from the complex, 25 mg of the raw product was injected into a HPLC column using an ion-free solvent system (solvent A, water; solvent B, methanol). The flow rate used was 5 mL/min with the following gradient: 10−55% B (1%/min). The peak eluting at 21.3 min was collected. The procedure was repeated until the whole sample was separated. The collected fractions were lyophilized to give 310 mg (60%) of a light brown solid and characterized by ^{1}H-NMR, FABMS, and microanalysis. Anal. Calcd (found) for $KGaC_{20}H_{16}N_4O_{10}S_2$: C, 36.77 (36.35); H, 3.70 (3.42); N, 8.58 (8.39); Ga, 10.7 (10.2); K, 5.98 (6.26); S, 9.81 (9.44). The ^{1}H-NMR spectrum showed two sets of signals of two isomers in a ratio of 1:0.81. Negative ion FABMS: *m*/*e* (relative abundance) 541 (100%).

Preparation of K[Ga(NDFFT)$_2$]·3H$_2$O (3b). Pure $Ga(OH)_3$ was prepared as described above using 83.6 mg (1.2 mmol) of gallium. To a slurry of purified $Ga(OH)_3$ in 5 mL of water was added a solution of 387.6 mg (1.6 mmol) of $NDFFTH_2$, **1b**, and 8.0 mL of 0.1 M KOH (0.8 mmol) in 10 mL of water. The resulting mixture was stirred for 36 h at room temperature. The solvent was removed, and the yellowish residue was applied to a Sephadex LH-20 column (25 × 1 cm) and eluted with methanol. The solvent was removed to give 323 mg (67%) of a yellow solid, which was characterized by ^{1}H-NMR, FABMS, and microanalysis. Anal. Calcd (found) for $KGaC_{18}H_{18}N_4O_9S_2$: C, 35.60 (35.35); H, 2.96 (2.93); N, 9.22 (8.90); Ga, 11.5 (12.1). The ^{1}H-NMR spectrum showed two sets of signals, indicating that there are two isomers in solution in a ratio of 1:0.59. Although separation of the two isomers was attempted by HPLC, using a flow rate of 5 mL/min and various solvent gradients, no separation was observed, again presumably due to interconversion. Negative ion FABMS: *m*/*e* (relative abundance) 514. The complex decomposes between 250 and 260 °C.

Preparation of Na[Co(DFFT)$_2$]·1.5H$_2$O (4a). $DFFTH_2$, **1a** (239 mg, 1.0 mmol), and 180 mg (0.5 mmol) of $Na_3[Co(CO_3)_3]\cdot 3H_2O$ were dissolved in 30 mL of water, and the mixture was stirred at room temperature for 18 h, during which the color changed from dark brown to reddish violet. The solvent was removed and the residue applied to a Chelex column (10 × 2 cm) and eluted with water. A brown band separated from the Co(II) impurities. After the solvent was removed, further purification was achieved by applying the red-violet solid to a Sephadex G-15 column (15 × 1 cm, eluent water) and afterward to a Sephadex LH-20 column (25 × 1 cm, eluent methanol). Lyophilization yielded 250 mg (91%) of the crude product as a violet solid. It was characterized by ^{1}H-NMR, FABMS, and microanalysis. Anal. Calcd (found) for $NaCoC_{20}H_{19}N_4O_{5.5}S_2$: C, 41.31 (41.60); H, 3.26 (3.60); N, 9.63 (9.01). The ^{1}H-NMR spectrum indicated that there are five different species in solution. The ratio of the isomers was determined to be 4.04:1.18:1.07:1. The last isomer could only be detected in trace amounts. Negative ion FABMS: *m*/*e* (relative abundance) 554 (90%). The complex is stable up to 350 °C.

Separation of the five isomers by HPLC was attempted; 30 mg of the isomer mixture dissolved in 0.2 mL of water was injected into the HPLC column using an ion-pairing solvent system (0.01 M NH_4OAc, pH 8.86) for both solvent A (water) and solvent B (methanol). The flow rate used was 5 mL/min with the following gradient: 10−20% B (2%/min); 20−30% B (1%/min); 30−45% B (1.5%/min); 45−55% (1%/min). Only the meridional isomers described previously[22] could be collected, as shown by ^{1}H-NMR measurements of the eluting peaks. The ratio of the isomers (A:C) was 1:1.26.

Preparation of Na[Co(NDFFT)$_2$]·3.5H$_2$O (4b). $NDFFTH_2$, **1b** (224 mg, 1.0 mmol), was dissolved in 30 mL of water, and 180 mg (0.5 mmol) $Na_3[Co(CO_3)_3]\cdot 3H_2O$ was added in small portions. The mixture was stirred for 24 h at room temperature, during which the solution changed from brown to red. The solvent was removed and the residue applied to a Chelex column (10 × 2 cm) and eluted with water to remove Co(II) impurities. The complex was further purified by chromatography on a Sephadex G-15 column (15 × 1 cm, eluent water) and on a Sephadex LH-20 column (25 × 1 cm, eluent methanol). Removal of the solvent followed by lyophilization yielded 200 mg (68%) of a dark red powder, which was characterized by ^{1}H-NMR,

Table 1. ^{1}H-NMR Data for $DFFTH_2$, **1a**, $NDFFTH_2$, **1b**, and Their Metal Complexes[a]

metal	isomer	CH_3 group	CH_2 group	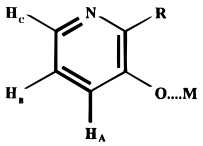	metal	isomer	CH_3 group	CH_2 group	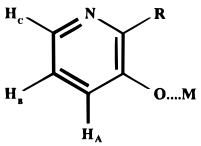
				$DFFTH_2$					
free ligand		1.71 ppm (s, 3H)	3.48 ppm (d, 1H) ^2J = 11.9 Hz 3.87 ppm (d, 1H)	a, b: 7.43 ppm (m, 2H) c: 8.04 ppm (dd, 1H) J_{AC} = 1.9 Hz J_{BC} = 3.9 Hz		*b*	1.62 ppm (s, 3H)	3.35 ppm (d, 1H) ^2J = 11.5 Hz 3.75 ppm (d, 1H)	a, b: 7.43 ppm (m, 2H) c: 8.05 ppm (dd, 1H) J_{BC} = 4.3 Hz J_{AC} = 1.3 Hz
Al^{3+}	A	1.72 ppm (s, 3H)	3.44 ppm (d, 1H) ^2J = 11.4 Hz 3.84 ppm (d, 1H)	a: 7.31 ppm (dd, 1H) J_{AB} = 8.7 Hz b: 7.48 ppm (dd, 1H) J_{BC} = 4.3 Hz c: 8.01 ppm (dd, 1H) J_{AC} = 1.3 Hz	Ga^{3+}	A	1.75 ppm (s, 3H)	3.45 ppm (d, 1H) ^2J = 11.5 Hz 3.84 ppm (d, 1H)	a: 7.34 ppm (d, 1H) J_{AB} = 9.5 Hz b: 7.47 ppm (dd, 1H) J_{BC} = 4.3 Hz c: 8.02 ppm (d, 1H) J_{AC} = 2.0 Hz
	C	1.75 ppm (s, 3H)	3.50 ppm (d, 1H) ^2J = 11.3 Hz 3.98 ppm (d, 1H)	a: 6.79 ppm (dd, 1H) J_{AB} = 8.7 Hz b: 7.25 ppm (dd, 1H) J_{BC} = 4.4 Hz c: 7.91 ppm (dd, 1H) J_{AC} = 1.3 Hz		C	1.77 ppm (s, 3H)	3.52 ppm (d, 1H) ^2J = 11.0 Hz 3.95 ppm (d, 1H)	a: 6.81 ppm (d, 1H) J_{AB} = 8.5 Hz b: 7.26 ppm (dd, 1H) J_{BC} = 4.5 Hz c: 7.92 ppm (d, 1H) J_{AC} = 2.2 Hz
				$NDFFTH_2$					
free ligand		3.71 ppm (dd, 1H) ^2J = 12.3 Hz	5.41 ppm (dd, 1H) ^3J = 6.2Hz	a: 7.45 ppm (d, 1H) J_{AB} = 7.5 Hz b: 7.54 ppm (dd, 1H) J_{BC} = 4.5 Hz c: 8.13 ppm (d, 1H) J_{AC} = 3.5 Hz	Ga^{3+}	C[c]	3.58−3.90 ppm (m, 2H)	5.49−5.62 ppm (m, 2H)	a: 6.84 ppm (dd, 1H) J_{AB} = 8.7 Hz b: 7.27 ppm (dd, 1H) J_{BC} = 4.3 Hz c: 7.93 ppm (dd, 1H) J_{AC} = 1.3 Hz
Al^{3+}	C[c]	3.61−3.92 ppm (m, 2H)	5.48−5.63 ppm (m, 1H)	a: 6.84 ppm (d, 1H) J_{AB} = 8.3 Hz b: 7.26 ppm (dd, 1H) J_{BC} = 4.1 Hz c: 7.92 ppm (d, 1H)		A[d]	3.70 ppm (dd, 1H) ^2J = 9.4 Hz 4.14 ppm (dd, 1H)	5.20 ppm (dd, 1H) ^3J = 5.3 Hz	a: 6.71 ppm (dd, 1H) J_{AB} = 7.3 Hz b: 7.13 ppm (dd, 1H) J_{BC} = 4.5 Hz c: 7.77 ppm (dd, 1H) J_{AC} = 1.4 Hz
	A[d]	3.70 ppm (dd, 1H) ^2J = 10.5 Hz 4.14 ppm (dd, 1H)	5.23 ppm (dd, 1H) ^3J = 7.4 Hz	a: 6.72 ppm (d, 1H) J_{AB} = 8.7 Hz b: 7.13 ppm (dd, 1H) J_{BC} = 4.0 Hz c: 7.78 ppm (d, 1H) J_{AC} = 1.4 Hz	Co^{3+}	A[c]	3.56 ppm (d, 1H) ^2J = 11.4 Hz 4.04 ppm (dd, 1H)	6.23 ppm (d, 1H) ^3J = 4.8 Hz	7.18−7.29 ppm (m, 3H)

[a] Proton NMR spectra were recorded in D_2O at 300 MHz. [b] Not separable by HPLC due to fast interconversion. [c] Some signals cannot be assigned because they are poorly resolved. [d] Solvent DMSO-d_6.

FABMS, and microanalysis. Anal. Calcd (found) for $NaCoC_{18}H_{19}N_4O_{9.5}S_2$: C, 36.69 (36.52); H, 3.22 (2.97); N, 9.50 (9.40). The ^{1}H-NMR spectrum showed only one set of signals, indicating only one isomer in solution. Negative ion FABMS: *m*/*e* (relative abundance) 526 (30%); 504 (100%).

Preparation of (Et$_3$NH)[Cr(NDFFT)$_2$]·CH$_3$COCH$_3$ (5b). To NDFFTH$_2$, **1b** (700 mg, 2.9 mmol), in 125 mL of acetone under argon were added 600 mg (1.6 mmol) of $CrCl_3$·3THF and 583 mg (5.8 mmol) triethylamine. The brown mixture was heated to reflux for 1 h and subsequently stirred at room temperature for an additional 15 h. The brown precipitate, removed by filtration, was identified as the triethylammonium salt. The solvent was removed in vacuo and the residue applied to a Sephadex LH-20 column (20 × 2 cm) and eluted with methanol. A yellow band was separated from the dark red residue. The solvent was removed in vacuo to yield 891 mg (93%) of the chromium complex. Anal. Calcd (found) for $CrC_{27}H_{34}N_5O_7S_2$: C, 49.40 (49.47); H, 5.18 (5.48); N, 10.66 (9.95); Cr, 7.48 (7.25). Negative ion FABMS: *m*/*e* (relative abundance) 496 (100%). The complex decomposes between 115 and 119 °C.

Isomer separation was achieved by HPLC using an ion-pairing system (0.01 M NH_4Ac, pH = 7.9) for both solvent A (water) and solvent B (methanol). A 5 mg quantity of the crude product dissolved in 0.15 mL water was injected into the HPLC column. The flow rate used was 5 mL/min with the following gradient: 9−38% B (5.3 %/min); 38−50% B (0.8%/min); 50−57% B (1%/min); 57−67% B (5%/min); 67−73% B (0.66%/min); 73−100% B (2.7%/min). Three, well-separated fractions could be collected at 40.3, 42.8, and 44.5 min. The solutions of the separated fractions were immediately placed in a cold bath of 2-propanol and dry ice and lyophilized. The first fraction gave a greenish powder, the second an orange solid, and the third a red solid. Approximately 15 mg of each fraction was applied to an AG 50W-X8 ion-exchange column (10 × 2 cm, K^+-form) and eluted with water. The collected fractions were again frozen and lyophilized. Final purification was achieved by chromatography on a Sephadex LH-20 column (20 × 2 cm, eluent methanol). The three fractions were characterized by vis/UV and CD measurements as well as by FABMS. First fraction: *m*/*e* (relative abundance) 496.1 (10%), 391.3 (42%), 277.1 (100%). Second fraction: 496.0 (56%), 409.0 (6%), 321.0 (12%). Third fraction: 496.0 (96%), 409.0 (12%), 391.2 (14%), 277.1 (100%). The CD and vis/UV measurements were also performed without chromatography of the separated fractions on an ion-exchange and a Sephadex column, giving the same results.

Preparation of K[Fe(DFFT)$_2$]·2.5 H$_2$O (6a). DFFTH$_2$, **1a** (239 mg, 1.0 mmol), was dissolved in 15 mL of water. A 5 mL portion of a 0.1 N KOH solution (0.5 mmol) and 176.6 mg (0.5 mmol) of ferric acetylacetonate were added, and the brown mixture was stirred at room temperature for 20 h. The color changed during this time from brown to deep red. The solvent was removed in vacuo. The residue dissolved in methanol was applied to a Sephadex LH-20 column (22 × 2 cm) and eluted with methanol. A yellow band could be separated from the ferric complex. The solvent was removed, to give 282 mg (92%) of a deep red powder. The sample was characterized by IR and vis/UV measurements, by FABMS, and by elemental analysis. Anal. Calcd (found) for $KFeC_{20}H_{21}O_{8.5}N_4S_2$: C, 39.22 (39.14); H, 3.43 (3.19); N, 9.14 (9.17); Fe, 9.60 (9.12). Negative ion FABMS: *m*/*e* (relative abundance) 528 (70%). The IR and vis/UV absorptions were similar to reported literature values.[13] The complex decomposes between 283 and 285 °C.

Preparation of K[Fe(NDFFT)$_2$]·2H$_2$O (6b). NDFFTH$_2$, **1b** (113 mg, 0.5 mmol), was dissolved in 10 mL of water and 2.5 mL of a 0.1 N KOH solution (0.25 mmol). An 88.3 mg (0.25 mmol) amount of ferric acetylacetonate was added, and the reddish reaction mixture was stirred for 48 h at room temperature. The color changed to dark reddish brown. The solvent was removed in vacuo, and the residue dissolved in methanol was applied to a Sephadex LH-20 column (22 × 2 cm) and eluted with methanol. The red band was collected, and the solvent was removed in vacuo to give 128 mg (89%) of a reddish powder which was characterized by FABMS, IR, and vis/UV techniques and by microanalysis. Anal. Calcd (found) for $KFeC_{18}H_{16}N_4S_2O_8$: C, 37.58 (37.87); H, 2.78 (2.67); N, 9.73 (9.70); Fe, 9.71 (9.56). Negative ion FABMS: *m*/*e* (relative abundance) 500 (80%). IR (KBr disk): 2690, 1655, 1632, 1597, 1428, 1329, 1188, 1096, 981, 808, 595 cm^{-1}. Vis/UV (MeOH, c = 54.4 μM), λ, nm (ϵ, M^{-1} cm^{-1}): 326 (16 800), 406 (5500), 460 (3900). The complex decomposes between 298 and 301 °C.

Table 2. Vis/UV and CD Spectral Data for [Co(NDFFT)$_2$]$^-$ and [Cr(NDFFT)$_2$]$^-$ Complexes in Methanol

	UV/vis		CD	
	λ_{max}, nm	ϵ, M^{-1} cm^{-1}	λ_{max}, nm	$\Delta\epsilon$, M^{-1} cm^{-1}
[Co(NDFFT)$_2$]$^-$ (isomer A)	506	638	510	4.68
	406	17340	470	1.81
	354	8511	432	15.21
	334	8830	390	−19.26
	292	7340	342	5.88
			320	2.53
			284	−11.60
[Cr(NDFFT)$_2$]$^-$ (fraction 1)[a]	543	242	767	−1.78
	375	6064	551	−5.19
	319	7500	385	16.28
	281	14043	335	−12.12
[Cr(NDFFT)$_2$]$^-$ (fraction 2)[a]	545	309	738	0.82
	377	8138	646	−1.41
	314	9096	549	2.69
	300	9415	455	−0.85
	288	8617	402	2.13
			358	−13.70
			314	5.11
			287	−3.64
[Cr(NDFFT)$_2$]$^-$ (fraction 3)[a]	538	287	773	−1.97
	380	7660	549	−4.76
	319	8298	399	17.02
	286	10452	354	−12.58
			306	3.99

[a] Fractions collected from HPLC.

Spectroscopic Measurements. Solutions of the pure isomers for vis/UV and circular dichroism spectroscopy were prepared of the following complexes: Na[Co(NDFFT)$_2$], **4b**, isomer A, 51.2 μM; K[Cr(NDFFT)$_2$], **5b**, fractions 1−3 (from HPLC), 46.7, 76.2, and 60.7 μM, respectively. Solutions were prepared in methanol to decrease the probability of isomerization. Concentrations were determined by atomic absorption. The maxima in absorbency were obtained by calculating derivative (dA/dλ) spectra. Spectroscopic data are summarized in Table 2.

X-ray Data Collection and Structure Solution and Refinement. Diffraction-quality crystals of K[Al(DFFT)$_2$]·2MeOH, **2a**, were obtained by vapor diffusion of diethyl ether into a solution of the separated isomer of **2a** in wet methanol at room temperature. A large specimen (0.55 × 0.40 × 0.40 mm^3) was mounted on a glass fiber and transferred onto an automatic Enraf-Nonius CAD4 diffractometer. Least-squares refinements of 24 reflections in the range 27.8° ≤ 2Θ ≤ 29.2° led to final cell constants. Using Mo Kα radiation and ω−2Θ techniques, a full hemisphere was collected (7795 reflections) in the range 3.0° ≤ 2Θ ≤ 45.0° at −105 °C. Data collection and refinement procedures were as earlier described.[26−28] No decay correction was performed (1.0% total loss of intensity), but an empirical absorption correction[26] was applied using Ψ-scan data (T_{max} = 0.998; T_{min} = 0.876). Structure and refinement parameters are given in Table 3. All hydrogen atoms were placed in calculated positions[27] and were constrained to ride on their respective carbon atoms. The enantiomeric structure with the expected *S* absolute configuration at C10 and C20 led to a better refinement result (R = 4.966%; R_w = 6.373%) than the alternative *R* absolute configuration (R = 5.033%; R_w = 6.429%). Full-matrix least-squares refinements with 344 variables and 2868 reflections (14 reflections were rejected) with $F_o^2 > 3\sigma F_o^2$ led to convergence with R = 3.57% and R_w = 3.75% and a GOF of 1.04. The maximum and minimum peaks of residual electron density are 0.656 and −0.225 e/Å^3. Selected bond distances and angles are presented in Table 4.

(26) *Structure Determination Package User Guide*; B. A. Frenz and Associates: College Station, TX 77840, 1982.
(27) Churchill, M. R. *Inorg. Chem.* **1973**, *12*, 1213.
(28) Harris, W. R.; Raymond, K. N.; Weitl, F. L. *J. Am. Chem. Soc.* **1981**, *103*, 2667−2675.

Table 3. Summary of Crystal Data for the Al Complexes

	$K[Al(DFFT)_2]\cdot 2CH_3OH$, **2a**	$K[Al(NDFFT)_2]\cdot 1.166H_2O\cdot CH_3OH$, **2b**
empirical formula	$KAlC_{22}H_{24}O_8N_4S_2$	$KAlC_{19}H_{18.33}O_{8.17}N_4S_2$
crystal size, mm^3	0.55 × 0.40 × 0.40	0.35 × 0.20 × 0.20
fw	602.62	563.60
a, Å	11.238(3)	21.269(8)
b, Å	31.719(11)	
c, Å	7.684(2)	9.643(3)
V, Å^3	2739.2(24)	3777.8(42)
space group	$P2_12_12$	$P6_1$
Z	4	6
d_{exp}, g/cm^3	1.48	1.50
d_{calc}, g/cm^3	1.46	1.48
μ_c, cm^{-1}	4.19	4.50
F(000)	1104	1560
transm factors	0.82−0.99	0.88−1.00
R	0.055	0.036
R_w	0.063	0.038

Table 4. Selected Bond Distances (Å) and Angles (deg) for the Al Complexes

	$K[Al(DFFT)_2]\cdot 2CH_3OH$, **2a**	$K[Al(NDFFT)_2]\cdot 1.166H_2O\cdot CH_3OH$, **2b**
	Distances	
Al−O1	1.832(2)	1.878(8)
Al−O2	1.961(2)	1.905(8)
Al−O4	1.815(2)	1.881(8)
Al−O5	1.961(3)	1.904(8)
Al−N2	1.964(3)	1.963(8)
Al−N4	1.947(3)	1.963(8)
	Angles	
O1−Al−O2	168.2(1)	167.2(3)
O1−Al−O4	93.6(1)	91.0(3)
O1−Al−O5	92.6(1)	90.6(3)
O1−Al−N2	89.4(1)	86.8(3)
O1−Al−N4	98.3(1)	91.8(4)
O2−Al−O4	92.1(1)	91.0(3)
O2−Al−O5	83.6(1)	89.8(3)
O2−Al−N2	79.7(1)	80.5(3)
O2−Al−N4	92.0(1)	100.9(3)
O4−Al−O5	168.4(1)	168.8(3)
O4−Al−N2	98.0(1)	96.4(3)
O4−Al−N4	98.6(1)	87.5(4)
O5−Al−N2	91.8(1)	94.8(4)
O5−Al−N4	79.9(1)	81.4(3)
N2−Al−N4	168.9(1)	175.9(4)

$K[Al(NDFFT)_2]\cdot 1.166H_2O\cdot MeOH$, **2b**, was crystallized by vapor diffusion of diethyl ether into a concentrated solution of **2b** (containing the mixture of isomers) in wet methanol at 4 °C. A suitable crystal (0.35 × 0.20 × 0.20 mm^3) was mounted on a glass fiber, and the structure analysis followed closely the one just described. Cell parameters were determined from least-squares refinements of 24 reflections in the range 21.4° ≤ 2Θ ≤ 24.5°; 3594 reflections ($+h,+k,\pm l$) were collected at −95 °C in the range 3.0° ≤ 2Θ ≤ 45.0°. The total loss of intensity for three check reflections was 1.2% over a period of 14.7 h. No decay correction was necessary, but an empirical absorption correction was applied using Ψ-scan data (T_{max} = 0.998; T_{min} = 0.819). Structure and refinement parameters are summarized in Table 3. There is a water molecule in the crystal that is disordered in the middle of a channel, built by potassium cations related by the 6-fold screw axis; it consequently has an occupancy of $^1/_6$. The total amount of water was confirmed by weight loss measurements of the crystals under vacuum. Selected bond distances and angles are shown in Table 4.

Solution Thermodynamics of $DFFTH_2$ and $NDFFTH_2$. Water was deionized and further purified by a Millipore system (resistivity 18 × 10^6 Ω·cm). The water was degassed by boiling and stored under argon prior to use. Stock KOH solutions were prepared from Baker Dilut-it standards and standardized against potassium hydrogen phthalate. Stock HCl solutions were also prepared from Baker Dilut-it standards and standardized against the KOH. All solutions were stored under an argon atmosphere.

Potentiometric titrations were performed with an automatic titrator (Metrohm 655 Dosimat automatic buret) and a Fisher Accumet pH meter with an Orion combination electrode. Water-jacketed vessels maintained at 25 ± 0.1 °C were used as reaction cells. Samples were typically 50 mL in volume and 0.8 mM in ligand concentration. The ionic strength was 0.1 N KCl. Potentiometric titrations were analyzed by using the program BETA90[28,29] to fit the pK_a values of $DFFTH_2$ and $NDFFTH_2$.

Spectrophotometric Titrations of the Gallium and Aluminum Complexes. Titrations were performed using a custom-built automatic titration device composed of an HP8450 vis/UV spectrophotometer connected to the automatic titrator described above, a 1 cm path length quartz cell, a Brinkmann Lauda K-2/R constant-temperature bath, and a computer equivalent to an IBM-XT. The BASIC program TIMBERWOLF[30] was used to control the titrator. Data analysis was achieved by REFSPEC,[31] a spectral componentization and nonlinear least-squares program, on an IBM-AT computer. The metal ion concentration used was about 0.04 mM, and the ligand concentration was about 0.08 mM. The ionic strength was 0.1 N KCl. In all titrations 2 mL of a 0.1 N HCl was added and the solutions were titrated from low to high pH.

Determination of the Stability Constants of the Iron Complexes. The pH titrations were performed using ethylenediaminetetraacetate (EDTA) as a competing ligand for iron. Due to slow equilibration, data sets could not be obtained by using the automatic titrator described above. Extinction coefficients of the $[Fe(DFFT)_2]^-$ and $[Fe(NDFFT)_2]^-$ complexes were determined at 440, 460, and 480 nm using five different concentrations. Twenty vials were arranged for both complexes, each containing 4 mL of 0.1 M KCl solution. To each of the first 20 vials (also 0.1 N in KCl) were added 200 μL of a 10.70 mM $FeCl_3$ solution, 2 mL of a 2.14 mM $DFFTH_2$ solution, and 213 μL of a 10.04 mM EDTA solution. To the second 20 vials were added 189 μL of a 10.70 mM $FeCl_3$ solution, 2 mL of a 2.03 mM $NDFFTH_2$ solution, and 201 μL of a 10.04 mM EDTA solution. The pH of both sets of vials was adjusted over a range from 2.5 to 6.5 with 0.1 M KOH using the same electrode as described in the preparation of the Al^{3+} and Ga^{3+} complexes. The color of the solutions ranged from orange at low pH to deep red at high pH. The vials were regularly shaken, and the absorbency of the solutions was monitored every 48 h. It was assumed that the equilibrium in both sets of vials had been reached when the absorbency remained constant 25 days after the vials were filled.

Electrochemistry of the Iron Complexes. Cyclic voltammetry was performed in water and in DMF using a BAS 100A electrochemical analyzer and a C-1 A/B cell stand. The samples were purged with argon before the measurements and were blanketed with argon during the acquisition. The cyclic voltammograms in DMF solution (Aldrich, anhydrous, 99+ %) were measured at a graphite working electrode with an ionic strength of 0.1 M ($(C_4H_9)_4NPF_6$ Sachem, electrochemical grade). The concentrations of $[Fe(DFFT)_2]^-$, **6a**, and $[Fe(NDFFT)_2]^-$, **6b**, were 1.11 and 0.98 mM, respectively. The potential was scanned at a rate of 10−50 mV/s from −0.300 to −1.300 V. The cyclic voltammograms are irreversible in this solvent; the anodic peaks of **6a** and **6b** were found at −0.863 and −0.792 V, respectively, versus the saturated calomel electrode (SCE). The differences in potential between the anodic and cathodic peaks were 132 and 120 mV. The measurements in water were performed in buffered solutions (pH 9.00 and 10.06, boric acid/borate, Aldrich, 99.999%) with an ionic strength of 0.1 M (KCl) at a carbon disk working electrode using a Ag/AgCl reference electrode. The concentration of Fe^{3+} was 1 mM, and the concentration of the ligands was 5 mM. The potential versus NHE was scanned from 0.000 to −0.600 V at various scan rates. The reductions of both ferric complexes in water are quasi-reversible; the separations of the anodic and cathodic peaks are 69 mV ($E_{1/2}$ = −97 mV) for **6b** and 104 mV ($E_{1/2}$ = −166 mV) for **6a**.

(29) Franczyk, T. S. Ph.D. Dissertation, University of California at Berkeley, 1991; pp 77−78, 112.
(30) Loomis, L. D. Ph.D. Dissertation, University of California at Berkeley, 1986.
(31) Turowski, P. N.; Rodgers, S. J.; Scarrow, R. C.; Raymond, K. N. *Inorg. Chem.* **1988**, *27*, 474−481.

Results and Discussion

Synthesis and Spectroscopic Characterization of the Complexes. General Information. Both ligands are tridentate and chiral. Therefore, in theory, five different pseudooctahedral complex isomers can be formed. In all isomers the two ligands are related by C_2 symmetry so that only one set of signals per isomer is observed in each ^{1}H-NMR spectrum. The three aromatic protons at the aromatic ring of each ligand form an ABC spin system. The two diastereotopic protons at the thiazoline ring give rise to an AM spin system for $DFFTH_2$ and an AMX system for $NDFFTH_2$. Therefore, a doublet of doublets for each isomer of $[M(DFFT)_2]^-$ and a doublet of quartets for $[M(NDFFT)_2]^-$ complexes should be observed.

Complexes of Gallium and Aluminum. The Ga and Al compounds were synthesized from excess $Al(OH)_3$ and $Ga(OH)_3$. After purification on a Sephadex LH-20 column, $[Ga(DFFT)_2]^-$, **3a**, $[Ga(NDFFT)_2]^-$, **3b**, and $[Al(NDFFT)_2]^-$, **2b**, show only two sets of signals in their ^{1}H-NMR spectra, corresponding to two isomers. In contrast, $[Al(DFFT)_2]^-$, **2a**, forms three isomers in solution in a ratio of 1:0.23:0.19; these are separable by HPLC into two fractions. The first fraction shows only one set of signals in the ^{1}H-NMR spectrum. This is the most abundant isomer from the mixture of isomers and was assigned as the A isomer via X-ray crystallography. The other fraction shows mainly one isomer (presumably isomer C) and smaller amounts of isomer A and a third, not characterized, isomer. Isomer A could be crystallized from methanol/diethyl ether whereas various attempts to crystallize the main isomer of the second fraction failed. As indicated by variable-temperature NMR spectroscopy, isomer A is stable and does not isomerize up to 95 °C in D_2O and 160 °C in DMSO-d_6. Attempts to separate the isomers of **3a**, **3b**, and **2b** by HPLC were not successful. When **2b** was crystallized from methanol/diethyl ether, using the mixture of the two isomers, only the A isomer was found in the crystals. Crystals of both Ga^{3+} complexes were obtained, but they were not suitable for X-ray data collection. In contrast to $[Al(DFFT)_2]^-$, the other three Ga(III) complexes isomerized very quickly after crystals of the compounds had been dissolved in D_2O, as indicated by NMR measurements. No isomerization occurred when the crystals of the pure isomers were dissolved in DMSO-d_6. This is consistent with a mechanism of isomerization that is proton dependent. (Note that **2a** is remarkably kinetically inert.) The ^{1}H-NMR data are listed in Table 1.

The Cobaltic Complexes. $Na_3[Co(CO_3)_3]$ was used as the starting material for the synthesis of the cobaltic compounds. The preparation of $[Co(DFFT)_2]^-$, **4a**, differed from that previously reported.[22] The ^{1}H-NMR spectrum of the reaction mixture taken after 18 h reaction time indicates that there are five different isomers in solution in a ratio of 4.04:1.18:1.07:1. One isomer could be detected only in trace amounts (Figure 3). By comparison of their chemical shifts, isomers 3 and 4 were assigned to be meridional isomers that were previously described.[22] Attempts to separate all five isomers by HPLC gave only both meridional isomers, with the C isomer slightly more abundant (1.26:1). In a second reaction, with a longer reaction time of 24 h, only the two meridional isomers could be detected. It would appear that the meridional isomers are thermodynamically much more stable than the kinetically favored facial isomers. This is why the main isomer could not be isolated by HPLC in the first reaction even though it had an abundance which was 4 times as high compared to those of the meridional isomers.

The reaction of $NDFFTH_2$ with $Na_3[Co(CO_3)_3]$ (surprisingly) gives only one isomer, whatever the reaction time. Unfortunately the signals in the aromatic region of the ^{1}H-NMR spectrum are so poorly resolved that no assignment is possible. The FABMS presents the final evidence that a 2:1 complex was formed, with the strongest peak at *m*/*e* 504 corresponding to $[Co(NDFFT)_2]^-$. The neutral complex $Na[Co(NDFFT)_2]$ could also be detected at *m*/*e* 526. The final assignment of this compound as the A isomer was achieved by vis/UV and CD spectroscopy (discussed later). This is in contrast to the case of $DFFTH_2$, where the C isomer is slightly more abundant.

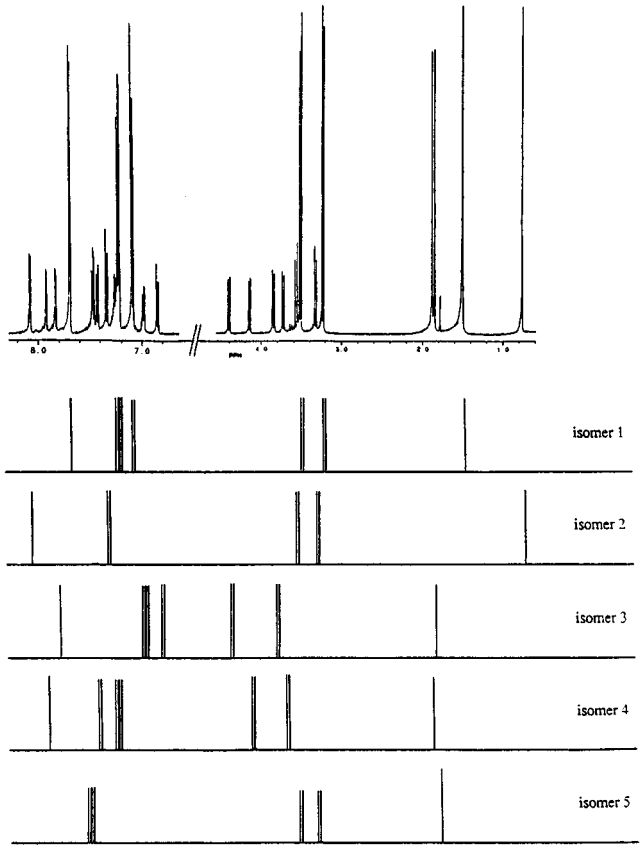

Figure 3. ^{1}H-NMR spectrum of $[Co(DFFT)_2]^-$, **4a**, in D_2O after a reaction time of 18 h and the schematic assignment of the five isomers.

The Chromic Complex of $NDFFTH_2$. The reaction of $NDFFTH_2$ with $CrCl_3 \cdot 3THF$ gave a dark red powder. Three well-separated bands could be collected from the HPLC column. The vis/UV spectra (Figure 5) of all three fractions are similar. All show the two spin-allowed transitions $^4A_{2g} \rightarrow {}^4T_{2g}$ (lower energy) and $^4A_{2g} \rightarrow {}^4T_{1g}$ (higher energy). The transitions at about 315 nm and lower presumably correspond to ligand absorption; they show distinct patterns for the second fraction but are almost identical for fractions 1 and 3. The CD spectra (discussed later) show the same similarity; it can be inferred from the data that fractions 1 and 3 represent the A isomer. This is consistent with the behavior of the Co^{3+} complex of $DFFTH_2$, where all five possible isomers have been observed. Attempts to separate the isomers, or a longer reaction time, led to the loss of the facial isomers. The Cr^{3+} isomers are separable, but the facial isomer also isomerizes very quickly, so that it cannot be characterized. Fraction 2 is assigned as the C isomer.

The Ferric Complexes. Although a preparation for $[Fe(DFFT)_2]^-$, **7a**, has been sketched,[32] we found it more effective to prepare small quantities of the complexes as described here. It is a straightforward synthesis with high yields. No separation of the different isomers of the ferric complexes has been achieved, presumably due to fast interconversion. Attempts to grow single crystals of the ferric complexes have also been unsuccessful, perhaps for the same reason.

(32) Peter, H. H.; Moerker, T. Eur. Pat. Appl. EP 325,559 (Cl. C07C83/00), July 26, 1989.

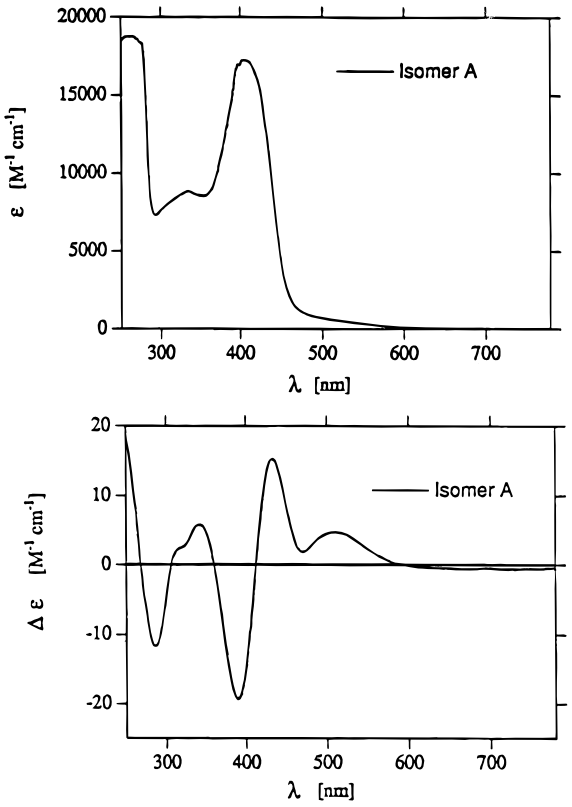

Figure 4. Vis/UV (upper panel) and CD (lower panel) spectra of $[Co(NDFFT)_2]^-$, **4b** (isomer A), in methanol.

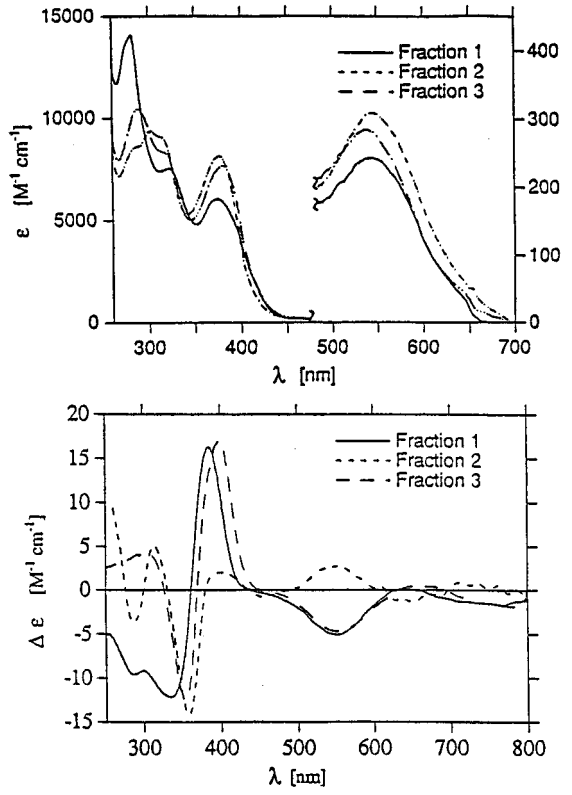

Figure 5. Vis/UV (upper panel) and CD (lower panel) spectra of the three fractions of $[Cr(NDFFT)_2]^-$, **5b**, separated by HPLC in methanol.

Structural Studies. The Al^{3+} complexes of both ligands were crystallized from methanol/diethyl ether. The salt $K[Al(NDFFT)_2]\cdot 1^1/_6H_2O\cdot MeOH$, **2b**, provides the first structure of the synthetic siderophore derivative $NDFFTH_2$. The geometry of the central Al^{3+} is pseudooctahedral in both complexes (Figure 6). Both compounds were crystallized as their potassium salts. The crystal data are summarized in Table 3. The

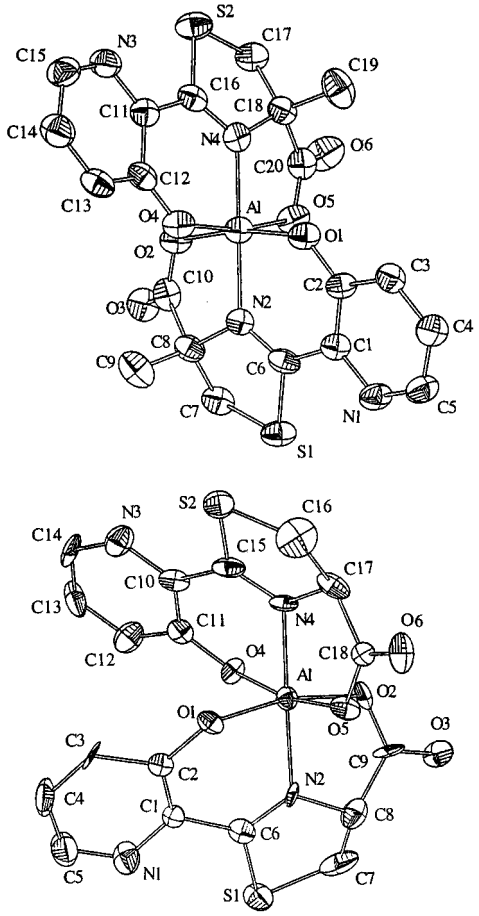

Figure 6. ORTEP diagrams of $[Al(DFFT)_2]^-$ (**2a**, upper) and $[Al(NDFFT)_2]^-$ (**2b**, lower).

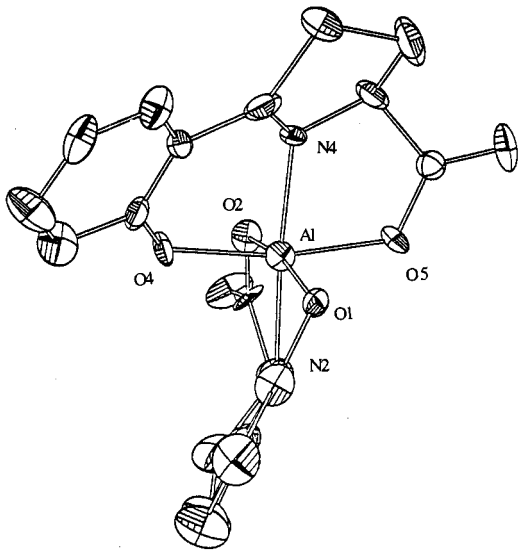

Figure 7. ORTEP diagram of **2b** showing the bent conformation of the ligands in the solid state.

absolute configuration of the chiral carbon atom in the ligand is *S* for **2a** and *R* for **2b**. The chirality at the metal center is in both complexes Λ; therefore, both structures represent the mer-(N,O-Λ) isomer. Both ligands coordinate to the metal with the phenolate oxygen atom, the nitrogen atom of the thiazoline ring, and the carboxylate oxygen atom. Both ligands are planar due to a delocalized π-system involving the hydroxypyridine ring, the double bond in the thiazoline ring, and the sulfur atom. This results in a distorted octahedral coordination geometry for Al in the complexes. As opposed to those of **2a**, the ligands of **2b** are not perpendicular to each other (Figure 7). The ligand

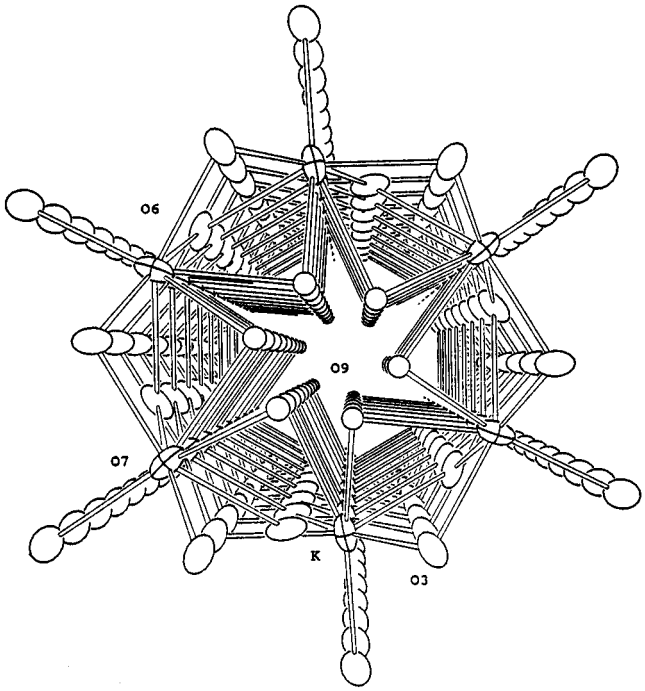

Figure 8. View along the channel formed by the 6-fold screw axis in the lattice of **2b**.

Table 5. Solution Thermodynamics of $DFFTH_2$, **1a**, and $NDFFTH_2$, **1b**[a]

	$DFFTH_2$		$NDFFTH_2$	
equilibrium	log *K*	p[M][b]	log *K*	p[M][b]
$L^{2-} + H^+ = LH^-$	9.75(3)		9.53(3)	
$LH^- + H^+ = LH_2$	3.26(8)		3.16(6)	
$LH_2 + H^+ = LH_3^+$	1.81(3)		1.95(20)	
$Al^{3+} + 2L^{2-} = [AlL_2]^-$	23.6(1)	14.7(1)	22.0(1)	13.5(1)
$[AlL_2]^- + H^+ = [AlL(LH)]$	6.6(1)		6.8(1)	
$[AlL(LH)] + H^+ = [Al(LH)_2]^+$	3.3(1)		3.7(1)	
$Ga^{3+} + 2L^{2-} = [GaL_2]^-$ [c]	29.2(3)	20.3(3)	27.8(2)	19.5(2)
$Fe^{3+} + 2L^{2-} = [FeL_2]^-$ [c]	31.04(3)	22.14(3)	29.09(3)	20.51(3)

[a] Constants were measured at 25 °C and 0.1 M (KCl) ionic strength. [b] pM values were calculated at pH = 7.4 using [M] = 1 μM and [L] = 10 μM. [c] No protonated species could be observed.

units remain planar while bending away from the N−Al−O plane. Selected bond distances and angles are presented in Table 4. The Al−N bond distances in both molecules are almost identical, at an average of 1.959 Å. The Al−O(carboxylate) distances are about 0.15 Å longer than the Al−O(phenolate) distances. The O1−Al−N4 angles are is 91.8° in **2b** and 98.3° in **2a**, and the O2−Al−N4 angles are 100.9 and 92.0°, respectively; these show how the ligands bend in **2b**. Compared with analogous distances in the structures of $[Cr(DFFT)_2]^-$,[22] the average bond distances in the aluminum complexes are 0.04−0.10 Å shorter, consistent with the 0.08 Å larger effective ionic radius of Cr^{3+} compared to Al^{3+}.[33] The structure of **2b** shows the same pattern. The bond angles of the Cr^{3+} and Al^{3+}-complexes are very similar.

Figure 8 presents a view along the 6-fold screw axis in the lattice of this complex. A channel is formed by potassium cations which are related by the screw axis.

Thermodynamic Results. Protonation Constants of $DFFTH_2$ and $NDFFTH_2$. Refinement of the potentiometric titration data using the computer program BETA90[28,29] gave three protonation constants for each ligand. The values are listed in Table 5. The values found here for $DFFTH_2$ are in good agreement with those earlier reported.[20] From high to low pH, protonation first takes place at the phenolate oxygen atom at the hydroxypyridine ring and then at the carboxylate oxygen atom. We assign the third protonation at the hydroxypyridine ring and not at the thiazoline ring (because of a possible hydrogen bond between the phenolic hydrogen atom and the nitrogen atom). The first two protonation constants of $NDFFTH_2$ are lower than those of $DFFTH_2$. This is surprising because $DFFTH_2$ seems to be otherwise a stronger base, in that it forms stronger complexes with all of the trivalent metal ions studied here. The third protonation constants of the two ligands are similar. In both compounds, $DFFTH_2$ and $NDFFTH_2$, the thiazoline ring decomposes in strong acid (to methylcysteine and cysteine, respectively); however $DFFTH_2$ decomposes much more slowly. To avoid decomposition, the solutions of the ligands were prepared just before the measurements.

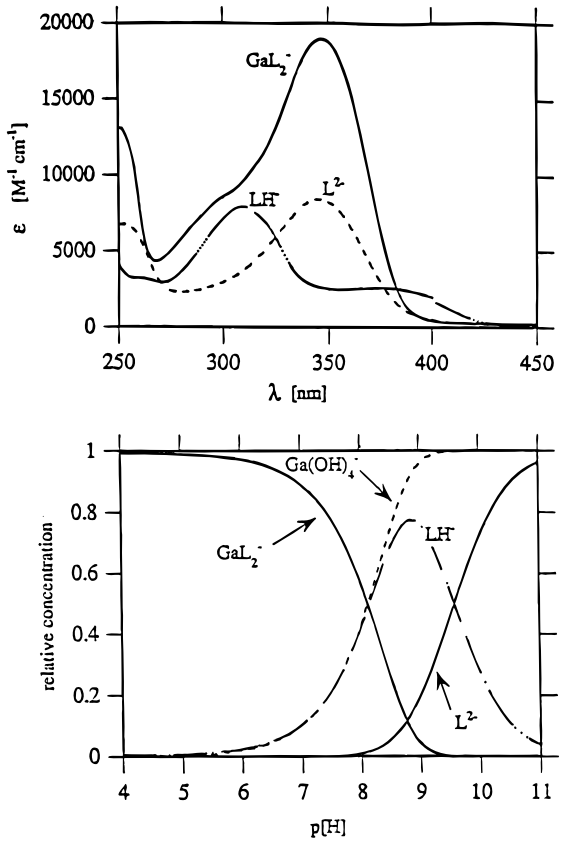

Figure 9. Calculated absorption spectrum (upper panel) and species distribution plot (lower panel) of the $[Ga(NDFFT)_2]^-$ titration. The total metal and ligand concentrations are 1 and 2 mM, respectively. Both ligands behaved similarly in the titration; therefore only the results for one ligand are displayed.

Stability Constants of $[M(DFFT)_2]^-$ and $[M(NDFFT)_2]^-$ (M = Al, Ga). The stabilities of the hydroxides (log *K*), as described by the reaction

$$M^{3+} + 4H_2O = [M(OH)_4]^- + 4H^+ \qquad (1)$$

are −25.6 for Ga^{3+} and −23.0 for Al^{3+}.[34] These are comparable to the stabilities of the siderophore complexes, so that the competition of OH^- and $DFFTH_2$ (or $NDFFTH_2$) for the metal ion could be used to measure the stability constant of the $[ML_2]^-$ complexes. A similar method was used to determine the stability of the Ga^{3+} complex of desferrioxamine.[35]

(33) Barnes, C. L.; Eng-Wilmont, D. L.; van der Helm, D. *Acta Crystallogr.* **1984**, *C40*, 922.
(34) Martell, A. E.; Smith, R. M. *Critical Stability Constants*; Plenum Press: New York and London, 1974; Vol. 1.
(35) Borgias, B.; Hugi, A. D.; Raymond, K. N. *Inorg. Chem.* **1989**, *28*, 3538−3545.

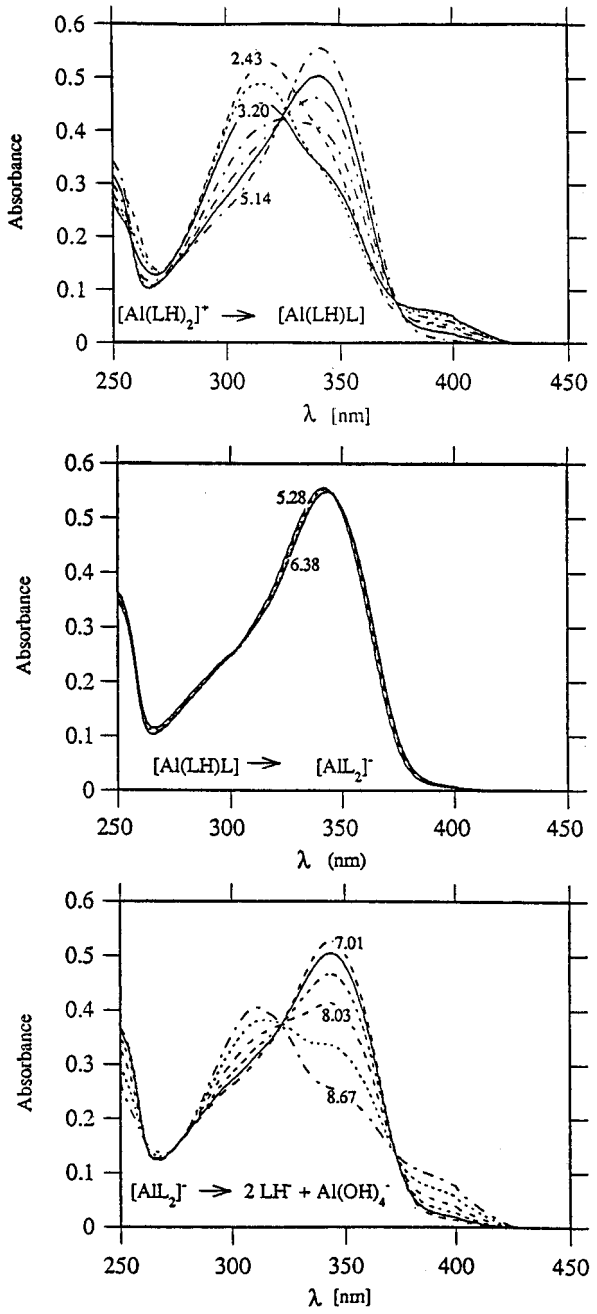

Figure 10. Family of vis/UV spectra generated by the pH titration of $[Al(NDFFT)_2]^-$: upper panel, pH 2.43−5.14; middle panel, pH 5.28−6.38; lower panel, pH 6.54−8.67.

In the spectrophotometric titration of the gallium complexes, only three absorbing species are observed. From pH = 2.9 to 9.0 the two absorbing species are the $[GaL_2]^-$ complex and the monoprotonated ligand LH^-. The gradual development of a shoulder at about 310 nm is accompanied by a decrease in absorbency at about 350 nm. This corresponds to the equilibrium

$$[GaL_2]^- + 4H_2O = [Ga(OH)_4]^- + 2HL^- + 2H^+ \quad (2)$$

From pH = 9.3 to 11.4 the absorption at about 310 nm decreases and the development of an absorption maximum at 345 nm (due to free ligand) is observed, due to the reaction

$$HL^- + OH^- = L^{2-} + H_2O \quad (3)$$

Figure 9 presents a calculated absorption spectrum and a species distribution of $[Ga(NDFFT)_2]^-$ (which behaves very similarly to $[Ga(DFFT)_2]^-$). Up to pH 6, Ga^{3+} is entirely complexed by the ligand, while at pH 8, only about 50% of the Ga^{3+} is still complexed by the siderophore. At even higher pH, $[Ga(OH)_4]^-$ is fully formed, leaving the deprotonated ligand in solution.

In the spectrophotometric titration of the aluminum complexes, the situation is more complicated (Figure 10). The following discussion describes the behavior of both compounds. Five different species are observed throughout the titration. From pH 3.2 to 5, development of an absorption at about 340 nm is observed. The corresponding reaction is

$$[Al(LH)_2]^+ = [Al(L)(LH)] + H^+ \quad (4)$$

The small change in absorption from about pH 5 to 6.5 corresponds to

$$[Al(L)(LH)] = [AlL_2]^- + H^+ \quad (5)$$

From pH 7 to 9, the $[AlL_2]^-$ complex is gradually lost, as indicated by a decrease of absorption at 340 nm and an increase at 310 nm, due to the reaction

$$[AlL_2]^- + 4H_2O = [Al(OH)_4]^- + 2LH^- + 2H^+ \quad (6)$$

The last step is the deprotonation of the ligand LH^- to give a final absorption maximum at 345 nm. This equilibrium is identical to eq 3. A species distribution for both Al^{3+} complexes and a calculated absorption spectrum for the species throughout the titration are plotted in Figure 11. The deprotonated $[ML_2]^-$ species are dominant at physiological pH, although while $[Al(DFFT)_2]^-$ is predominant in this pH range, only about 70% of the $[Al(NDFFT)_2]^-$ is formed. The decomposition of $[AlL_2]^-$ into $[Al(OH)_4]^-$ occurs at pH 9 for $DFFTH_2$ and at pH 8 for $NDFFTH_2$. The stability constants and pM values of the complexes are listed in Table 5. The constant reported here for $[Al(DFFT)_2]^-$ is slightly higher than found earlier.

Stability Constants of $[Fe(DFFT)_2]^-$ and $[Fe(NDFFT)_2]^-$. In the determination of the equilibrium constant for the reaction

$$[FeL_2]^- = Fe^{3+} + 2L^{2-} \quad (7)$$

the EDTA complex with a stability constant (log *K*, reaction 8) of 25.1[36] was used as a competitor. The equilibrium of the competition reaction

$$[FeL_2]^- + EDTA^{4-} = [FeEDTA]^- + 2L^{2-} \quad (8)$$

is very slow.

$$K_e = [FeEDTA^-][L^{2-}]^2/[FeL_2^-][EDTA^{4-}] \quad (9)$$

The concentration of FeL_2^- was obtained directly from the vis/UV absorptions (between 430 and 500 nm), since no other species in this reaction absorbs in this range. The resultant stability constants and corresponding pM values are listed in Table 5. The constant for $[Fe(DFFT)_2]^-$ is somewhat higher than reported earlier. The only significant species at physiological pH is the $[FeL_2]^-$ complex (L = DFFT, NDFFT).

Circular Dichroism Spectra. The Vis/UV and corresponding CD spectra of $[Cr(NDFFT)_2]^-$ (fractions 1−3 from HPLC) are presented in Figure 5. The order of energy states for Cr^{3+} (d^3) is $^4A_{2g} < {}^4T_{2g} < {}^4T_{1g}$, with the lower energy manifold ($^4A_{2g} \rightarrow {}^4T_{2g}$) at about 540 nm and the higher energy transition ($^4A_{2g}$

(36) Harris, D. C. *Quantitative Chemical Analysis*, 3rd ed.; W. H. Freeman Co.: New York, 1987.

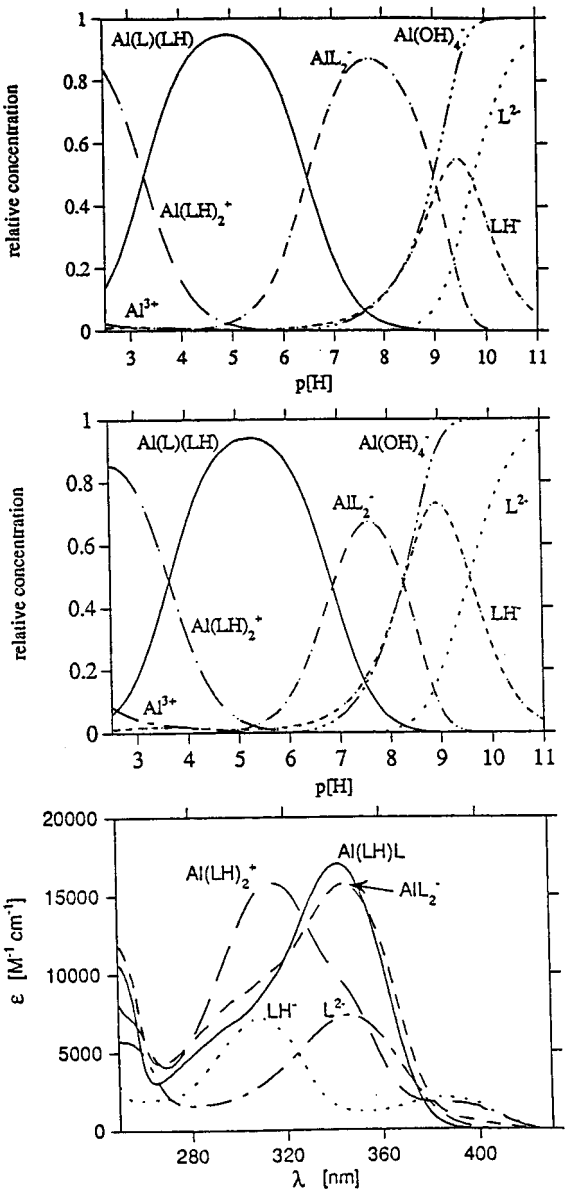

Figure 11. Species distribution plots for $DFFTH_2$ (upper panel) and $NDFFTH_2$ (middle panel) and a calculated absorption spectrum of the species in the $[AlL_2]^-$ titration (lower panel). The total metal and ligand concentrations are 1 and 2 mM, respectively.

$\rightarrow {}^4T_{1g}$) at about 370 nm.[37] The other absorptions at higher energy are assigned as ligand absorptions. The spectra of all three fractions are similar. The CD spectra of fractions 1 and 3 show comparable patterns. The weaker transition of the lower energy manifold (800−500 nm) and the stronger absorption of the higher energy manifold (420−360 nm) have the same sign whereas the bands in the CD spectrum of fraction 2 are opposite in sign at lower energy and have the same sign at higher energy. The same rationalization used earlier in assigning the spectra for DFT complex applies here.[22] In comparison with previously reported spectral data, fractions[22] 1 and 3 are A isomers. The order of energy states in the Co^{3+} (d^6) complex ($^1A_{1g} < {}^1T_{1g} < {}^1T_{2g}$) gives the same symmetries for the transition as for the Cr^{3+} complex and very similar spectra, as shown in Figure 4.

Cyclic Voltammetry. Cyclic voltammograms were measured in water and in anhydrous DMF. Both ferric complexes show quasi-reversible waves in water. The reduction potentials of $[Fe(DFFT)_2]^-$, **6a**, and $[Fe(NDFFT)_2]^-$, **6b**, are −166 and −97 mV, respectively, versus NHE (50−200 mV/s). The lower potential of **6a** parallels its higher stability constant. Both reduction potentials are accessible by biological reductants.[7] For a Nernstian system, the potential is given by $E = 0.770 - 0.059(\log \beta_{III} - \log \beta_{II})$, where β_{III} and β_{II} are the cumulative stability constants of the ferric and the ferrous complexes ML_2. This gives values for $\log \beta_{II}$ of 15.2 for $[Fe^{II}(DFFT)_2]$ and 14.4 for $[Fe^{II}(NDFFT)_2]$. The cyclic voltammograms recorded in anhydrous DMF show waves with peak separations of about 130 mV. The reduction potentials are −595 mV for **6a** and −524 mV for **6b** (versus NHE). Neither an increase in ligand concentration nor the addition of base (NEt_3) gave reversible reduction waves.

Summary Comparison of Desferriferrithiocin ($DFFTH_2$) and Nordesferriferrithiocin ($NDFFTH_2$). Several complexes of $NDFFTH_2$ and $DFFTH_2$ with Fe^{3+} or similar ions have been prepared and characterized in this study. All five possible isomers of $[Co(DFFT)_2]^-$ are observed whereas only one isomer of $[Co(NDFFT)_2]^-$ is formed. Three isomers are found for $[Al(DFFT)_2]^-$ and $[Cr(NDFFT)_2]^-$ but only the two meridional isomers could be fully characterized. For the other complexes, only the meridional isomers have been found. The facial isomers are kinetically favored in the reactions studied but are thermodynamically unstable. For all of the complexes (except $[Al(DFFT)_2]^-$) only the meridional isomers are detected, if the reaction time is long enough. In general, the A isomer (mer-{N,O-Λ}) has a higher abundance in solution than the C isomer (mer-{N,O-Δ}) and is the most stable isomer in the solid state, for both ligands. For each of the complexation equilibria studied, the natural siderophore, $DFFTH_2$, forms slightly stronger complexes than its synthetic analog, always by about 1.5 orders of magnitude.

Acknowledgment. A Rotary Foundation scholarship to K.L. is gratefully acknowledged. S.R. and D.H. thank the Deutsche Forschungsgemeinschaft for postdoctoral fellowships. We thank Professor Alex von Zelewsky for his help regarding the nomenclature of the isomers. This research was supported by NIH Grant AI11744.

Supporting Information Available: Tables of positional and anisotropic thermal parameters, bond distances and angles, and root-mean-square amplitudes of thermal vibration and two fully labeled plots of **2a** and **2b** (16 pages). Ordering information is given on any current masthead page.

IC9601854

(37) Mason, S. F. *Molecular Optical Activity and the Chiral Discriminations*; Cambridge University Press: Cambridge, U.K., 1982.